SCA-9823

DIFFUSION IN INTERNAL FIELD GRADIENTS

Gigi Qian Zhang, George J. Hirasaki and Waylon V. House

Rice University

Abstract

The similarity of the values of NMR surface relaxivity of sandstones has led to the adoption of a default value of the T_2 irreducible water saturation cut-off for all sandstones. Chlorite coated sandstones should be treated as an exception since the T_2 distribution is strongly dependent on the echo spacing.

Chlorite coated North Burbank sandstone shows a much stronger diffusion effect due to internal field gradients on NMR T_2 measurements compared to Berea sandstone. This can also result in a shortened relaxation time for the oil phase, which can be mistaken as a wettability change. North Burbank sandstone has a T_1/T_2 and ρ_2/ρ_1 that is larger than most values reported in the literature.

A series of experiments on chlorite and kaolinite powderpacks with a variety of fluids were performed. There is clear evidence of strong internal magnetic field gradients in chlorite/fluid systems. This gradient is due to the high magnetic susceptibility contrast between chlorite and pore fluids. Kaolinite has a low magnetic susceptibility due to absence of iron and thus shows much less gradient effect. Not only the type of clay, but also how the clay is distributed in rocks, determines the extent of the gradient and diffusion effects on T_2 measurements. Chlorite is particularly important because this clay is often paramagnetic and lines the pore walls. The significance of the effect of diffusion due to internal field gradients depends on the magnitude of this effect compared to the relaxation rate due to bulk fluid relaxation and surface relaxation.

Introduction

NMR well logging is finding wide use in formation evaluation. Due to logging speed requirements, NMR CPMG T_2 measurements are used to estimate formation parameters like porosity, permeability, and capillary bound water. The T_2 relaxation process of fluids inside porous medium is a complex one. Besides the surface relaxation process, T_2 relaxation also has contributions from bulk relaxation and diffusion relaxation mechanisms.

Recently, a number of papers focused on the NMR relaxation by diffusion in the presence of a magnetic field gradient. Most of the studies are based on an applied magnetic field gradient rather than on internal field gradients. This is because the latter is dependent on the details of the pore geometry and mineralogy, which is either unknown or too complex to model [(Glassel and Lee, 1974), (Bendel, 1990), (Kleinberg and Horsfield, 1990), (Jerosch-Herold, et al., 1991), (Bobroff and Guillot, 1996)]. Brown and Fantazzini (1993) used a model of multiple correlation times to study a τ-dependent increase in the value of $1/T_2$ obtained from CPMG measurements. LaTorraca et al. (1995) used the NMR diffusion theory of Bergman et al. (1995) for analyzing the effects of internal field gradients on the T_2 relaxation rate.

Although the diffusion effect on NMR T_2 measurement has been recognized (Kenyon, 1997), iron-rich chlorite coated sandstones have not been singled out as exceptionally susceptible to internal gradient effects. However, from our T_1, T_2 measurements of different types of sandstones, we discovered that chlorite coated North Burbank sandstone showed significant departures from default assumptions about sandstone response (Zhang, et al., 1998). In the present paper, we focus on diffusion in internal field gradient of systems with chlorite.

Berea and North Burbank Sandstones

Berea and North Burbank sandstones were selected to evaluate the diffusion effect due to internal gradients. Table 1 compares their properties. They have similar porosity and permeability, but are very different because of the type of clays. Berea is moderately shaly and the clays are primarily book-like kaolinite and needle-like illite (Shell Rock Catalog). North

Burbank is chamosite coated (Trantham, 1977). A common feature of the chamosite is that it is an iron-rich chlorite and it is pore lining. The photomicrograph of a North Burbank sand grain showing chlorite coating at 10,000 magnification and a view of clays in Berea at 2000 magnification are shown in Fig. 1. NMR T_1 and T_2 measurements were performed in triplicate for sandstones saturated with brine and different hydrocarbons. Due to good reproducibility, the relaxation time distribution from only one sample of each sandstone will be illustrated.

The surface relaxivity, T_1/T_2, and T_2 cutoff for the sandstones studied here were reported previously (Zhang, et al., 1998). The values of these parameters for the North Burbank sandstone differed significantly from the values considered typical for sandstones.

Soltrol 130 is a refined aliphatic oil with a narrow range of molecular weights. It has a narrow, log normal T_1 distribution with a log mean value of 864 ms. SMY is the code name of a turbidite formation, deep water Gulf of Mexico, 30° API crude oil. This crude oil has a broad relaxation time distribution. The interactions of these fluids in different sandstones were discussed in an earlier publication (Zhang, et al., 1998).

NMR Measurements

All NMR measurements reported here were made with a MARAN-2 spectrometer. The T_1 measurements were made with the inversion recovery method with 50 measurements between 0.01 ms and 10,000 ms. The T_2 measurements were made with the CPMG method with the indicated echo spacing. The T_1 and T_2 measurements had a wait time between repetitions and a data acquisition time equal to 4-6 times the longest relaxation time.

Diffusion Effect on Soltrol with Brine at S_{wir}

The effect of internal gradient is illustrated by displaying the T_1, T_2 (TE=0.2 ms), and T_2 (TE=2 ms) distributions for Berea, Fig. 2, and North Burbank, Fig. 3, partially saturated with Soltrol and brine at S_{wir}. The log mean value of the T_1 distribution for bulk Soltrol is also shown as the vertical line. The peak at long relaxation times corresponds to Soltrol, and the broad peak at short relaxation times corresponds to the capillary bound water.

Clearly there is little difference between the T_1 and T_2 distributions for Berea and the Soltrol peak is near its bulk position. The behavior of Berea sandstone with Soltrol/brine provides the common case of negligible diffusion effect on T_2 measurements due to internal gradients.

However, North Burbank is very different. The relaxation time distributions of the capillary bound water at 100% brine saturation and at S_{wir} (Zhang, et al., 1998) can be explained by the microchannel model proposed by Straley et. al (1995) and interpretations of diffusional coupling by Ramakrishnan, et al. (1998). For T_1 distribution, the Soltrol peak appears at its bulk position. T_2 measurements at short echo spacing (TE=0.2 ms) show all peaks shifting to shorter times with the Soltrol peak far away from its bulk position. When echo spacing increases to 2 ms, the distributions shift further to shorter times, and flatten out. This shortening of the hydrocarbon peak is not due to wettability alteration because it would also have affected the T_1 distribution. Since the measurements were done in a laboratory spectrometer without an applied field gradient, it is concluded that there is a strong diffusion effect due to internal gradients for North Burbank sandstone with Soltrol/brine.

Diffusion Effect on SMY Crude Oil with Brine at S_{wir}

The North Burbank sandstone was cleaned, saturated to 100% brine saturation and centrifuged in SMY crude oil to S_{wir}. Its T_1, T_2 (TE=0.2 ms), and T_2 (TE=2 ms) distributions are shown in Fig. 4. The distribution for the bulk SMY crude oil, scaled to the oil saturation, is also shown for comparison.

Unlike the Soltrol/brine system that has separate peaks for Soltrol 130 and brine at S_{wir}, the T_1, and T_2 distributions for the SMY crude oil/brine system have crude oil and brine responses that overlap. It is observed that the brine peak for the Soltrol/brine system (Fig. 3) and the crude oil/brine system appears at the same position and is of the same magnitude for both T_1 and T_2 measurements. Therefore, the crude oil response and brine response can be qualitatively distinguished. The brine peak in the crude oil/brine system shifts to the same extent with echo spacing as the brine peak in the Soltrol/brine system. This is because brine exhibits the same

extent of diffusion effect since it stays inside the microchannels formed by chlorite flakes lining the pore walls of the North Burbank sandstone. However, the extent of echo spacing dependent shortening for the crude oil peak in the crude oil/brine system is much less compared with the shortening of the Soltrol peak in Soltrol/brine system. This will be discussed later.

Magnetic Susceptibility

The internal field gradient is proportional to the volume susceptibility, χ, contrast between rock grains and pore fluid (Kleinberg, 1996). Specific magnetic susceptibility, ψ, for various substances was measured and their values were converted to χ through the density (Table 2).

Paramagnetic materials have positive χ values, while diamagnetic materials have negative χ values. As shown in the table, siderite and hematite have the highest magnetic susceptibility values. Other minerals that contain iron also have higher χ values than iron-free minerals. The liquids have negative χ values, i.e. they are diamagnetic.

Berea contains siderite, so there is only a factor of 2.6 between the χ values of North Burbank sandstone and Berea sandstone. However, they have significant differences in diffusion effects due to internal gradients. This could be because the siderite in Berea is localized as cluster of crystals while the drusy chlorite in North Burbank pervasively coats the pore walls. Only the fluids in the vicinity of the paramagnetic minerals are affected by the internal gradients. Therefore, not only the type of paramagnetic mineral, but also how the mineral is distributed, determines the extent of the diffusion effect on T_2 measurements.

There is about a factor of 6.7 between the χ value of pure chlorite and that of North Burbank sandstone. Thus, it is reasonable to expect a stronger diffusion effect with pure chlorite compared to North Burbank sandstone. An iron-free clay, kaolinite, which exists in Berea, is chosen as an example of a diamagnetic clay.

Internal Field Gradients of Chlorite and Kaolinite Powderpack/Fluid Systems

Four liquids: 5% NaCl brine, hexane, Soltrol 130 and SMY crude oil were selected. Each chlorite or kaolinite powderpack was first mixed with an excess of liquid, left to settle for a couple of hours, and the excess bulk liquid removed. T_1 and a series of T_2 measurements with increasing echo spacing were performed on these powderpack/fluid systems using a MARAN-2 (2 MHz) spectrometer with a homogeneous applied magnetic field.

BET surface area was measured for the chlorite and kaolinite powders using the COULTER SA 3100 analyzer. The pore volume per unit clay weight in clay/fluid system is measured in brine. Assuming the pore structures in clay/fluid systems are cylindrical, the average pore radius can be calculated from the following equation:

$$r = 2\frac{v}{s} \tag{3}$$

where v is pore volume per unit weight and s is surface area per unit weight. The results are shown in Table 3.

Relaxation Time Distributions

T_1, T_2 distributions at different echo spacing are shown for the chlorite/fluid systems in Fig. 5, and for the kaolinite/fluid systems in Fig. 6. The T_1 distributions for bulk fluids are also displayed for comparison. The shift of the T_1 distribution of the clay/fluid system from the T_1 distribution of the bulk fluid is due to surface relaxation. The strongest surface relaxation effect is observed with brine as the fluid. The echo spacing dependent shortening of T_2 relaxation reflects the diffusion effect due to internal field gradient. All chlorite/fluid systems have greater diffusion effects compared to the corresponding kaolinite/fluid system. Of the chlorite/fluid systems, chlorite/crude oil exhibits the smallest diffusion effect

The diffusion effect due to internal field gradient observed with the chlorite powderpack is greater than that observed with the North Burbank sandstone. The latter is only chlorite coated and has larger macropores. Kaolinite has much less diffusion effect than chlorite.

Correlation of $1/T_2$ with τ^2

In an infinite medium with uniform gradient, the dependence of $(T_2)^{-1}$ on τ^2 is linear (Kenyon, 1997). The mechanism for T_2 relaxation can be expressed by the following three terms:

$$\frac{1}{T_2} = \frac{1}{T_{2B}} + r_2 \frac{S}{V} + \frac{1}{3}(tgG)^2 D \quad (1)$$

where τ is half of the echo spacing, γ is the nuclear gyromagnetic ratio, G is the gradient of the magnetic field, and D is the diffusivity of the fluid.

Figure 7 plots $1/T_2$ vs. τ^2 for chlorite/fluid systems. T_1 relaxation rate is shown at zero τ^2 with a square marker. The smallest echo spacing is 0.2 ms, and increases to 2 ms. For each chlorite/fluid system, the first several points fit very well to a straight line, while points at larger τ^2 deviate from it, apparently due to restricted diffusion effects. This line, when extrapolated to zero τ^2, does not necessarily intercept at the T_1 relaxation rate, possibly due to the difference between T_1 relaxivity, ρ_1 and T_2 relaxivity, ρ_2, at zero echo spacing. Alternatively, there may be a change in slope for echo spacing less than 0.2 ms.

The correlation between $1/T_2$ and τ^2 for the kaolinite/hexane system is shown in Fig. 8, and for the kaolinite/Soltrol system is similar. Since kaolinite/fluid systems have less diffusion effect than chlorite/fluid systems, experiments were performed with larger echo spacing up to 20 ms. The common feature of these two systems is that experimental points fit to a straight line below 2 ms TE, then deviate from this line, and finally reach a plateau.

The magnitude of the internal field gradient can be calculated from the slope of the line fitted to the first few points on a $1/T_2$ vs. τ^2 plot. The γ value of a proton is $2.675 * 10^8$ $Tesla^{-1}$ s^{-1}. The diffusivity of n-hexadecane is used to approximate that of Soltrol 130, because they have similar T_1 distributions.

The internal field gradients G for chlorite/fluid systems are compared to those of kaolinite/fluid systems in Table 4. Chlorite/fluid systems have G values that are an order of magnitude greater than those of kaolinite/fluid systems. Also, they are much greater than the applied gradient of logging tools.

Correlation of $1/T_2$ with τ

Bergman et al. (1995) used a Fourier expansion method to solve the diffusion eigenvalue problem associated with T_2 relaxation in a periodic porous medium. Based on their theory, LaTorraca et al. (1995) interpreted the effects of internal gradients on laboratory T_2 measurements. They correlated the relaxation rate due to diffusion with half of echo spacing using the following hyperbolic tangent function:

$$\Delta Rate = A(1 - \tanh(lt)/lt) \quad (2)$$

where A and λ are fitting parameters. A proportional relationship between λ and diffusivity and pore size did not appear to exist for our clay/fluid systems.

Model for Magnetic Field between Clay Flakes

It is well accepted that the internal field gradient is caused by the magnetic susceptibility difference between rock grains and pore fluid, and the relationship is usually expressed as following (Kleinberg, 1996):

$$G \approx \frac{\Delta B}{R} \approx \frac{\Delta c B_0}{R} \quad (4)$$

where R is the distance over which the magnetic field varies. However, a realistic physical model has not been proposed to account for this correlation.

For chlorite coated sandstones, chlorite flakes can be viewed as forming microchannels perpendicular to the pore walls such that each micropore opens to the macropore (Fig. 9(a)) (Straley, 1995). The magnetic fields in macropores, micropores and chlorite flakes were modeled between two planes of symmetry parallel to the magnetic field lines (Fig. 9(b)). Due to the paramagnetic characteristics of chlorite, field lines are concentrated inside the chlorite flake, while the magnetic field strength in the micropore is weakened. If end effect and transition region

are ignored, the magnetic field strength of the macropore, B_o, micropore, B_f and inside the chlorite flake B_c can be calculated. The magnitude of B_f is:

$$B_f = \frac{(1 + c_f)B_0}{1 + c_c + (c_f - c_c)x_c} \quad (5)$$

where x_c represents the dimension (fraction) of the microchannel, χ_f is the volume susceptibility of the fluid and χ_c is that of chlorite. The greatest magnetic field difference between macropore and micropore is about 100 ppm of B_o when the size of the microchannel becomes small compared to the size of the chlorite flake.

Since $\chi_c + (\chi_f - \chi_c)\, x_c << 1$, from Taylor's series expansion, Eq. (5) becomes:

$$\Delta B = B_0 - B_f \cong \Delta c\ B_0 (1 - x_c) \quad (6)$$

Therefore, the internal field gradient is

$$G \approx \frac{\Delta B}{R} \cong \frac{\Delta c\ B_0 (1 - x_c)}{R} \quad (7)$$

with

$$G_{max} \approx \frac{\Delta c\, B_0}{R} \quad (8)$$

which gives the same expression as Eq. (4).

Table 5 lists the G_{max} values calculated for chlorite and kaolinite/fluid systems assuming R equals to the pore radius determined from Eq. (3) and listed in Table 3. The order of magnitude of these values is consistent with the measured values in Table 4. G_{max} for chlorite/fluid systems are significantly higher than those of kaolinite/fluid systems.

An alternative model is to have the chlorite lined pore wall parallel to the magnetic field. In this case the field strength will be greater in the micropores than in the macropores. Manuscript limitations do not permit discussion of this model.

Relative Contributions of Different Mechanisms

Within the same North Burbank sandstone, brine, Soltrol and SMY crude oil exhibit different extents of shifting due to internal field gradients, Fig. 3 and Fig. 4. T_1 and T_2 relaxation of fluids in porous media have different mechanisms. The total T_1 relaxation rate is the summation of two terms:

$$\frac{1}{T_1} = \frac{1}{T_{1B}} + \frac{1}{T_{1S}} \quad (9)$$

while the total T_2 relaxation rate is the summation of three terms:

$$\frac{1}{T_2} = \frac{1}{T_{2B}} + \frac{1}{T_{2S}} + \frac{1}{T_{2D}} \quad (10)$$

where $1/T_{iB}$ (i=1,2) is the bulk fluid relaxation rate, $1/T_{iS}$ (i=1,2) is the surface relaxation rate, and $1/T_{2D}$ is the rate due to diffusion.

The tabulated values of each term in total T_1 andT_2 relaxation rates are available from the authors. Here, mode values are used to represent the corresponding T_1 and T_2 relaxation time distributions instead of log mean values, because SMY crude oil has a broad and skewed relaxation time distribution. For T_1 measurements, surface rate is calculated by subtracting bulk rate from total rate. For T_2 measurements, surface relaxation rate is assumed to be equal to the T_1 surface rates. Diffusion rate is then determined by subtracting bulk rate and surface rate from total rate. (Alternatively, the T_2 surface rate could have been determined as the difference between the relaxation rate extrapolated to zero τ^2 and the bulk fluid relaxation rate. However, this resulted in negative diffusion rates for the shortest relaxation times.)

For the chlorite/brine system, surface rate is dominant in T_1 measurement, while it is of the same order of magnitude as diffusion rate for T_2 measurement at short (0.2 ms) echo spacing. But when echo spacing increases to 2 ms, the diffusion rate becomes dominant. The patterns for the chlorite/hexane system and the chlorite/Soltrol system are similar to each other.

Both the bulk rate and surface rate are of similar magnitude and are relatively small. So, even for T_2 at short echo spacing, the diffusion rate is dominant. For the chlorite/crude oil system, bulk rate becomes important because of the fast relaxation of bulk crude oil compared to hexane and Soltrol. The diffusion rate for the crude oil system is small for T_2 measurement at short echo spacing. This is due to the small diffusivity value of this 30° API gravity crude oil (the diffusivity is approximately proportional to the bulk fluid relaxation time), and the bulk rate is of the same order of magnitude as the diffusion rate. But when echo spacing increases to 2 ms, diffusion rate becomes dominant, even for the crude oil. This analysis of the relative contributions of the three relaxation mechanisms is consistent with the extent of surface relaxation and diffusion effect observed from Fig. 5.

For the kaolinite/brine system, surface rate is dominant in T_1 measurement, while it is of the same order of magnitude as diffusion rate both for T_2 measurement at short echo spacing and at long echo spacing. For the kaolinite/hexane system, bulk rate becomes important. Even for T_2 at long echo spacing, it is of the same importance as the diffusion rate. For the kaolinite/Soltrol system, bulk rate is always the dominant rate in total T_1 and T_2 relaxation rates. For the kaolinite/crude oil system, the three rates almost have the same significance. In conclusion, for all these kaolinite/fluid systems, diffusion effect is small due to the low magnetic susceptibility value of kaolinite, and it is often masked either by bulk relaxation or surface relaxation.

Conclusions

There is very little internal gradient effect on T_2 measurements for Berea sandstones with a 2 MHz spectrometer. However, even at an echo spacing as small as 0.2 ms, a strong diffusion effect due to internal field gradient is observed on North Burbank sandstone saturated with Soltrol 130 and brine at S_{wir}, while much less diffusion effect is observed on the crude oil/brine system. Experiments on chlorite powderpack/fluid systems show even stronger diffusion effects. An iron-free clay, kaolinite, has much less diffusion effect. This demonstrates that iron-rich clays induce strong internal field gradients due to their high magnetic susceptibility. However, not only the type of clay, but also how the clay is distributed in rocks, determines the extent of diffusion effect on T_2 measurements. Chlorite needs special attention because of its high magnetic susceptibility and pervasive lining of pore walls.

Pore lining chlorite can be modeled as clay flakes forming microchannels perpendicular to pore walls such that each micropore opens to a macropore. The internal field gradient for such systems can be calculated using the model proposed in this paper. It gives results similar to those determined from a $1/T_2$ vs. τ^2 plot.

The significance of the diffusion effect due to internal field gradients depends on the relative magnitude of this effect compared with the relaxation rate due to bulk fluid relaxation and surface relaxation. SMY crude oil, with its low diffusivity and high bulk relaxation rate does not have a significant diffusion effect compared to hexane or Soltrol.

Diffusion in internal field gradients results in T_2 shortened relative to T_1. This is of significance to NMR well logging when estimating the wait or recovery time between pulse train repetitions, estimating T_2 cutoff, and estimating wettability effects.

Acknowledgments

The authors wish to acknowledge the financial support of an industrial consortium of Arco, Exxon, GRI, Mobil, Norsk Hydro, NUMAR, Saga, Schlumberger, Shell, and Western Atlas. The authors thank Exxon for magnetic susceptibility measurements, Shell for core sample preparation, Phillips for North Burbank samples, the Rice Geology Department for the kaolinite sample, and Western Atlas for the chlorite sample.

References

Bendel, P., "Spin-Echo Attenuation by Diffusion in Nonuniform Field Gradients", *J. Magn. Reson*., (1990), v. 86, 509.

Bergman, D. J., Dunn, K. J., and LaTorraca, G. A., "Magnetic susceptibility contrast and fixed field gradient effects on the spin-echo amplitude in a periodic porous medium with diffusion", *Bull. Am. Phys. Soc.*, (1995), 40, 695.

Bobroff, S. and Guillot, G., "Susceptibility Contrast and Transverse Relaxation in Porous Media: Simulations and Experiments", *Magn. Reson. Imaging*, (1995) v. 14, no. 7/8, 819.

Brown, R. J. S. and Fantazzini, P., "Conditions for initial quasilinear T_2^{-1} versus τ for Carr-Purcell-Melboom-Gill NMR with diffusion and susceptibility differences in porous media and tissues", *Phys. Rev. B*, (1993), v 47, 14823.

Glasel, J. A. and Lee, K. H., "On the Interpretation of Water Nuclear Magnetic Resonance Relaxation Times in Heterogeneous Systems", *J. Am. Chem. Soc*., (1974), v. 96:4, 970.

Jerosch-Herold, M., Thomann, H., and Thompson, A. H., "Nuclear Magnetic Resonance Relaxation in Porous Media", SPE 22861 prepared for presentation at the 66th ACE of SPE, Dallas, TX, October 6-9, 1991.

Kenyon, W. E., "Petrophysical principles of application of NMR logging", *The Log Analyst*, (1997), March-April, p. 21-43.

Kleinberg, R. L. and Horsfield, M. A., "Transverse Relaxation Processes in Porous Sedimentary Rock", *J. Magn*. *Reson*., (1990), v. 88, 9.

Kleinberg, R. L. and Vinegar, H. J., "NMR properties of reservoir fluids", *The Log Analyst*, (1996), Nov.-Dec..

LaTorraca, G. A., Dunn, K. J., and Bergman, D. J., "Magnetic susceptibility contrast effects on NMR T_2 logging", SPWLA 36th Annual Logging Symposium, June 26-29, 1995, p. 1-4JJ-.

Ramakrishnan, T.S., Schwartz, L. M., Fordham, E. J., Kenyon, W. E., and Wilkinson, D. J., "Forward Models for Nuclear Magnetic Resonance in Carbonate Rocks", SPWLA 39th Annual Logging Symposium, Keystone Resort, CO, May 26-29, 1998.

Straley, C., Morriss, C. E., Kenyon, W. E., and Howard, J. J., "NMR in partially saturated rocks: laboratory insights on free fluid index and comparison with borehole logs", *The Log Analyst*, January-February, 1995, p. 40-56.

Trantham, J. C. and Clampitt, R. L., "Determination of oil saturation after waterflooding in an oil-wet reservoir - The North Burbank Unit, Tract 97 Project", *J. Pet. Technol.*, (1977), 491-500.

Zhang, Q., Lo, S.-W., Huang, C.C., Hirasaki, G.J., Kobayashi, R., and House, W.V., 1998, "Some Exceptions to Default NMR Rock and Fluid Properties", 39th Annual Symposium of SPWLA, May 26-29, 1998, Keystone Resort, CO.

Table 1 Rock properties		
Rock name	Berea	North Burbank
Clays (%)	3%	Chlorite coated
Porosity (%)	18.9±0.8	23.1±1.0
Permeability (md)	205±20	237±64

Table 2 Magnetic susceptibility			
Substance	Formula	Specific Magnetic Susceptibility (ψ,10^{-6} cgs/g)	Volume Susceptibility (χ, 10^{-6})
Siderite	$FeCO_3$	77.2	305.8
Hematite	Fe_2O_3	49.7	261.2
Chlorite		35.5	104.6
Glauconite		26.1	69.8
Goethite	αFeO·OH	21.7	82.5
North Burbank		6.0	15.7
Berea		2.4	6.1
Bentheim		-0.14	-0.36
Kaolinite	$Al_2Si_2O_5(OH)_4$	-0.34	-0.90
Distilled Water	H_2O	-0.70	-0.70
Brine	5%NaCl	-0.73	-0.75
n-hexane	C_6H_{14}	-0.86	-0.56
Soltrol 130		-0.79	-0.59
Filtrate of OBM		-0.88	-0.69

Table 3 BET estimate of pore dimensions		
	chlorite	kaolinite
BET surface area, s (m^2/g)	1.331	6.369
Pore volume, v (cm^3/g)	0.493	1.337
Pore radius, r (μm)	0.741	0.420

Table 4 Internal field gradients (Gauss/cm) from fitting of $1/T_2$ vs. τ^2 plot			
	Brine	Hexane	Soltrol
Chlorite	270.9	187.4	544.4
Kaolinite	13.58	6.42	22.5

Table 5 Maximum internal field gradients (Gauss/cm) from $G_{max} = \frac{\Delta c B_0}{R}$			
	Brine	Hexane	Soltrol
Chlorite	711	710	710
Kaolinite	1.8	4.0	3.7

Fig. 1 (a) Photomicrograph of North Burbank sand grain showing chlorite coating (X10,000) (Trantham, et al., 1977) (b) View of clays in Berea. “Book-like” kaolinite and “needle-like” illite (X2000) (Shell Rock Catalog).

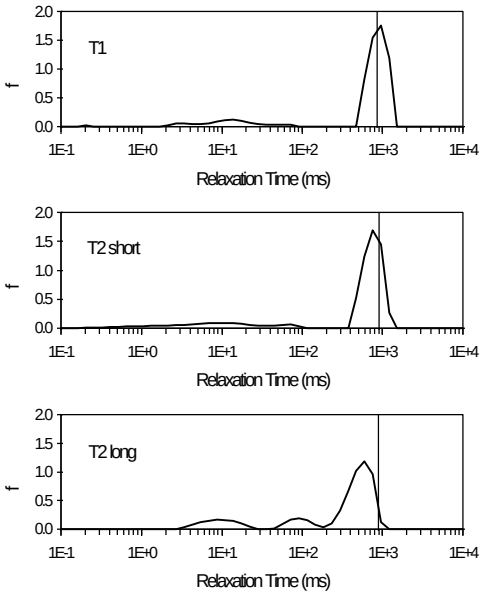

Fig. 2 Relaxation time distributions of T_1, T_2 (TE=0.2 ms), and T_2 (TE=2 ms) of Soltrol with brine at S_{wir} in Berea sandstone.

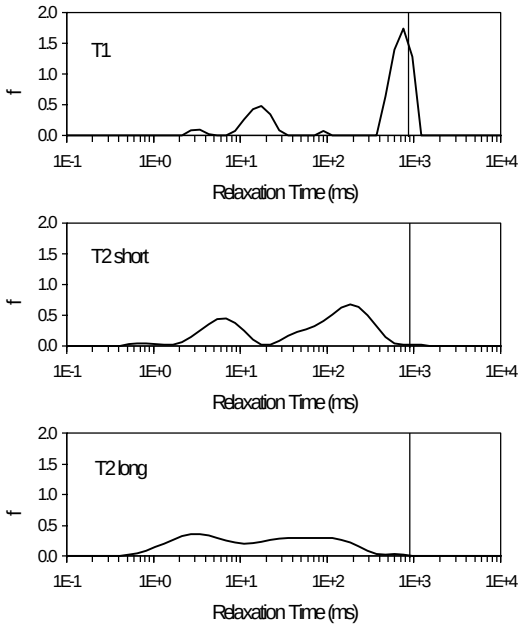

Fig. 3 Relaxation time distributions of T_1, T_2 (TE=0.2 ms), and T_2 (TE=2 ms) of Soltrol with brine at S_{wir} in North Burbank sandstone.

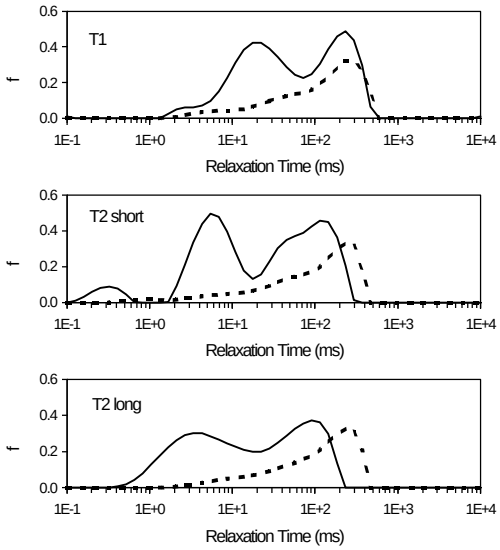

Fig. 4 Relaxation time distributions of T_1, T_2 (TE=0.2 ms), and T_2 (TE=2 ms) of SMY/brine (solid curve) in North Burbank sandstone compared to bulk oil (dotted curve) scaled to oil saturation.

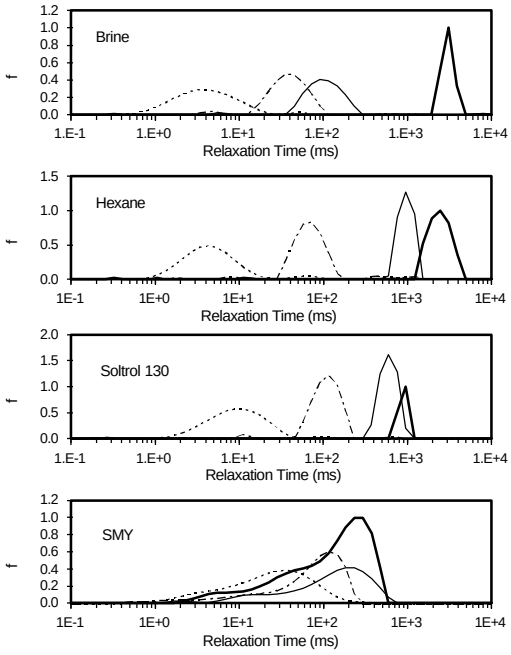

Fig. 5 Relaxation time distributions of T_1 (regular solid curve), T_2 (TE=0.2 ms) (dashed curve), and T_2 (TE=2 ms) (dotted curve) of chlorite/fluid systems. T_1 distribution of bulk fluid is shown as the bold solid curve.

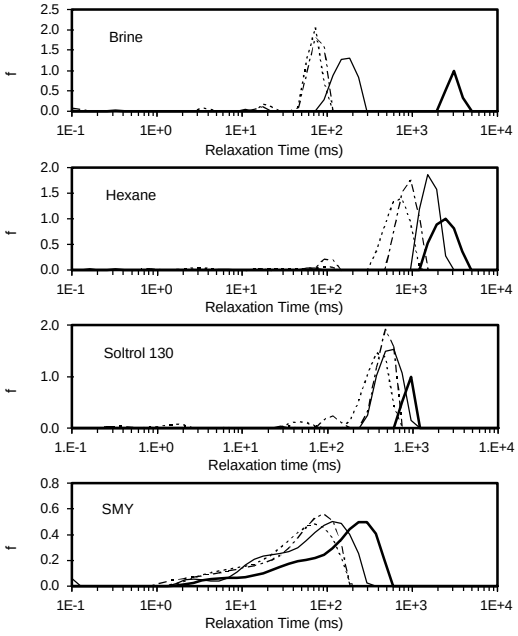

Fig. 6 Same as Fig. 5 except with kaolinite/fluid systems.

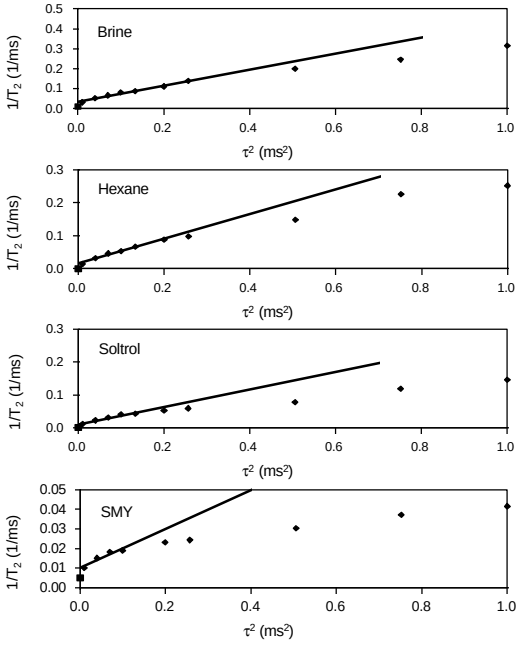

Fig. 7 Correlation of $1/T_2$ with τ^2 for chlorite/fluid systems. Square markers represent the T_1 relaxation rate.

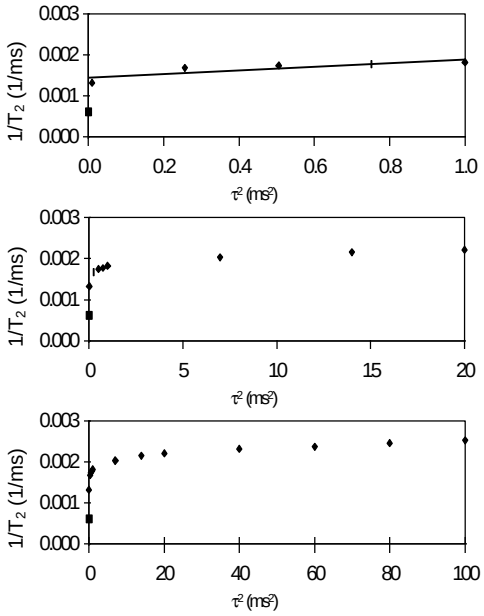

Fig. 8 Correlation of $1/T_2$ with τ^2 for kaolinite/hexane system with increasing scale. Square markers represent the T_1 relaxation rate.

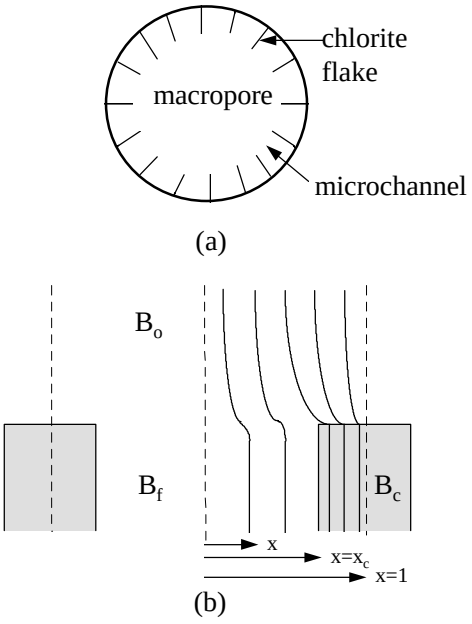

Fig. 9 Model of magnetic field for chlorite coated sandstone. (a) chlorite flakes forming microchannels open to macropore; (b) magnetic fields of macropore, B_o, micropore, B_f and inside chlorite flake, B_c.